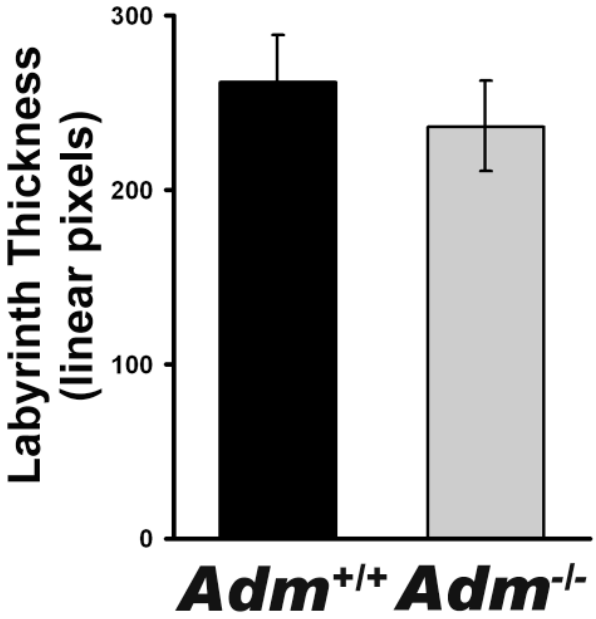

Supplemental Figure 1 Thickness of the labyrinth layer as measured from the chorionic plate to the spongiotrophoblast layer in *Adm*$^{+/-}$ and *Adm*$^{-/-}$ e13.5 placentas shows no significant difference.

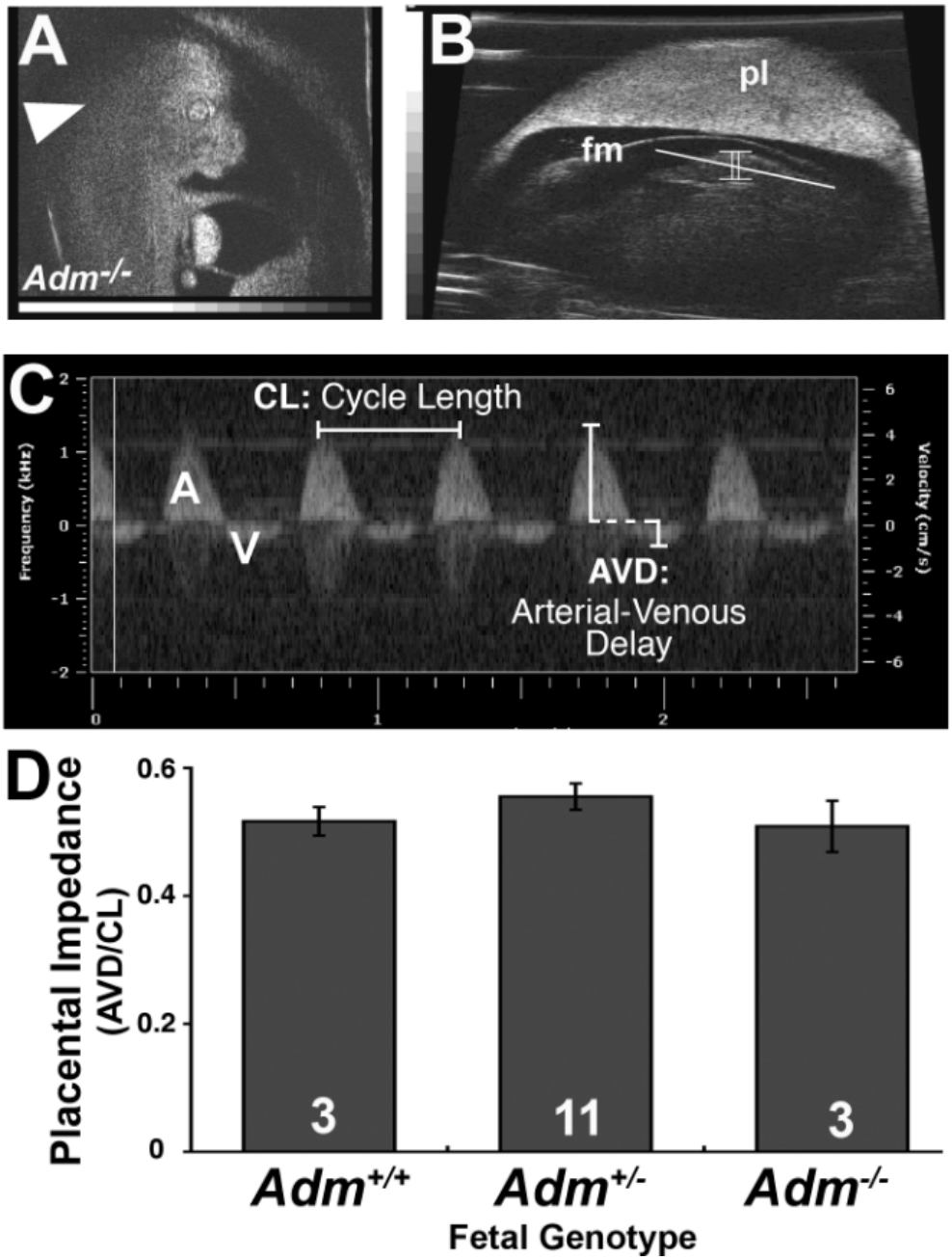

Supplemental Figure 2 Intravital Doppler Ultrasound for evaluation of placental function. (**a**) Doppler image of *Adm*$^{-/-}$ embryo at e13.5, revealing characteristic embryonic edema (white arrowhead). (**b**) Doppler image of placenta (pl) and fetal membranes (fm). Probe was centered on the umbilical cord for rendering Doppler wave forms (highlighted by bars). (**c**) M-mode tracings of umbilical card blood flow, showing both umbilical artery (A) and umbilical vein (V) frequencies and velocities. The relative vascular resistance of the placental vascular bed is described by placental impedance, which is calculated by dividing the arterial-venous delay (AVD) by the cycle length (CL). (**d**) Placental impedance was not significantly affected by the fetal genetic dosage of *Adm*. Numbers in the bars represent N. Data are expressed as mean +/- s.e.m.

Supplemental Figure 3 Gene expression profile of trophoblast and placental markers. To determine whether there were any changes in the differentiation or population of different placental and trophoblast cell types, we developed quantitative RT-PCR primers and probes for a variety of cell-specific markers. Consistent with the high expression of *Adm* in P-TGCs and the co-localization of apoptosis to the P-TGC region, the P-TGC-specific marker placental lactogen 1 (PL1) was significantly reduced in *Adm*$^{-/-}$ placentas compared to wildtype placentas. N of at least 10 placentas were analyzed for each genotype. Data are expressed as mean +/- s.e.m. * P < 0.05 by Student's t test.

Supplemental Figure 3: Gene expression profile of placental marker genes in e13.5 *Adm*$^{-/-}$ placentas

Gene	Placental cell type / layer	Primer and Probe Sequences	Percent Change Relative to *Adm*$^{+/+}$
Hand1	Trophoblast Giant Cells (P-TGC, S-TGC, SpA-TGC, C-TGC)	Forward: 5'-ggatgcacaagcaggtgac-3' Reverse:5'-ctcgagaaggcatcagggtact-3' Probe: 5'-FAM-tcgtccccttcttggctctgcg-TAMRA-3'	130 +/- 37
Prl2c2 (Proliferin-1) *(Plf)*	Trophoblast Giant Cells (P-TGC, SpA-TGC, C-TGC)	Forward: 5'-caagccaggctcacacacta-3' Reverse:5'-gatcgtccagagggctttcc-3' Probe: 5'-FAM-tgaaatcaggagccatgattttggatgc-TAMRA-3'	117 +/- 26
Prl3d1 (placental lactogen 1) *(Pl1)*	Trophoblast Giant Cells (P-TGC)	Forward: 5'-ggtgccgagttgtctttcaga-3' Reverse:5'-ccatgtgggcagggctt-3' Probe: 5'-FAM-cgaatgttgagtgcccacccagc-TAMRA-3'	73* +/- 6
Tpbpa	Spongiotrophoblast and Glycogen trophoblasts	Forward: 5'-ggagtggcctcagctgctat-3' Reverse:5'-cttctttatcttctgctcttgc-3' Probe: 5'-FAM- ccctgaagcgcagttggatgctg-TAMRA-3'	138 +/- 29
Mash2	Spongiotrophoblast	Forward: 5'-ctccgcctactcgtcggag-3' Reverse:5'-ctggaaaagtcaagcagctcct-3' Probe: 5'-FAM-ctgcgagggagagctaagcccgat-TAMRA-3'	106 +/- 12
Gcm1	Labryinth (chorionic trophoblasts and syncytiotrophoblast layer II cells)	Forward: 5'-gaggcacgacggacgct-3' Reverse:5'-tctccggcctgggatga-3' Probe: 5'-FAM-atctttttccgtccaaaggcgagca-TAMRA-3'	48* +/- 9
JunB	Labryinth and Spongiotrophoblast and Trophoblast Giant Cells	Forward: 5'-tacttttcgggtcagggatca-3' Reverse:5'-gcgctccagttccgtgg-3' Probe: 5'-FAM-acacaggcgcatctctgaagctagcc-TAMRA-3'	78* +/- 15
Gab1	Labyrinth and Spongiotrophoblast	Forward: 5'-atttccaccgtggatttgaac-3' Reverse:5'-gatctatcgctcggaaaggtc-3' Probe: 5'-FAM-ttgcggaaagatgctagttctcaagattgc-TAMRA-3'	65* +/- 7

P-TGC=parietal trophoblast giant cell; SpA-TGC=spiral artery TGC; S-TGC=maternal sinus TGC; C-TGC=Canal-associated TGC

* $p < 0.05$

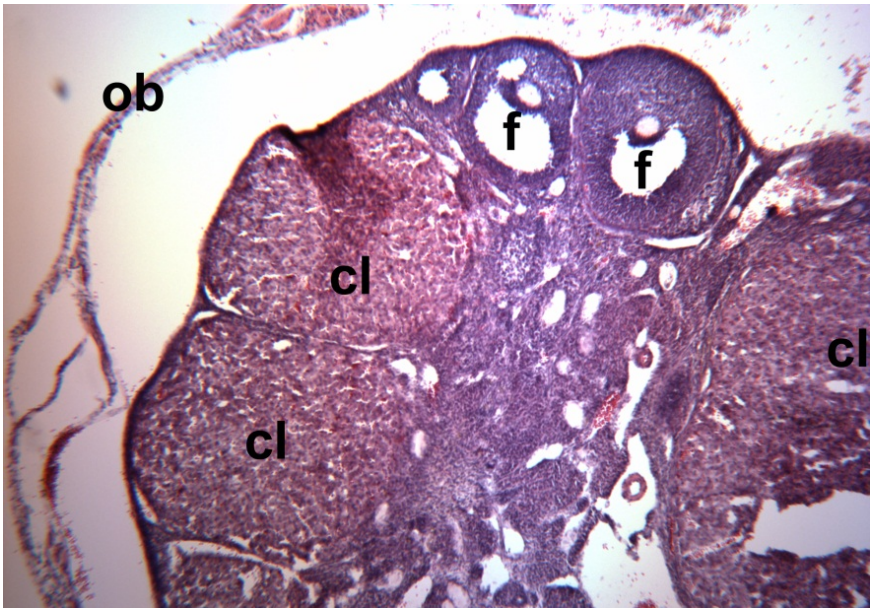

Supplemental Figure 4 H&E staining of transplanted *Adm*$^{+/-}$ ovary in an *Adm*$^{+/+}$ recipient after successful pregnancy. Note the anatomical retention of the transplanted ovary within the ovarian bursa (ob). Also evident are numerous ovarian follicles (f) at various stages of development and several corpora lutea, indicative of successful pregnancy and estrogenic function.

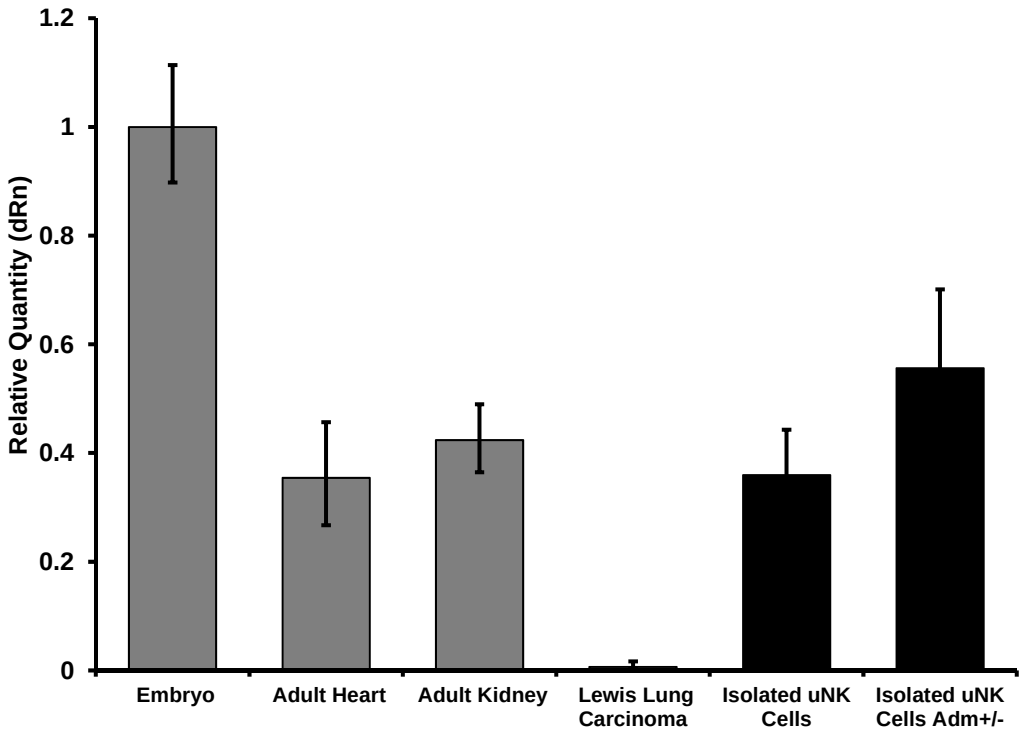

Supplemental Figure 5 Relative expression levels of *Calcrl* in various mouse tissues and cell lines, normalized to levels present in total embryo RNA. As expected, levels of *Calcrl* are high in vascularized tissues, including adult heart and kidney. Levels of *Calcrl* are relatively high and equivalent in uNK cells isolated from either wildtype or $Adm^{+/-}$ female mice. Lewis Lung Carcinoma cell line, which we have previously shown expresses little to no *Calcrl* and is unresponsive to AM signaling, serves as a negative control.